
PERGAMON

Neural Networks 15 (2002) 1085–1098

Neural Networks

www.elsevier.com/locate/neunet

2002 Special Issue

Image denoising using self-organizing map-based nonlinear independent component analysis

Michel Haritopoulos*, Hujun Yin, Nigel M. Allinson

Department of Electrical Engineering and Electronics, UMIST, P.O. Box 88, Manchester M60 1QD, UK

Abstract

This paper proposes the use of self-organizing maps (SOMs) to the blind source separation (BSS) problem for nonlinearly mixed signals corrupted with multiplicative noise. After an overview of some signal denoising approaches, we introduce the generic independent component analysis (ICA) framework, followed by a survey of existing neural solutions on ICA and nonlinear ICA (NLICA). We then detail a BSS method based on SOMs and intended for image denoising applications. Considering that the pixel intensities of raw images represent a useful signal corrupted with noise, we show that an NLICA-based approach can provide a satisfactory solution to the nonlinear BSS (NLBSS) problem. Furthermore, a comparison between the standard SOM and a modified version, more suitable for dealing with multiplicative noise, is made. Separation results obtained from test and real images demonstrate the feasibility of our approach.

Keywords: Self-organizing maps; Independent component analysis; Nonlinear; Image denoising; Multiplicative noise

1. Introduction

One of the increasingly important tools in signal processing is independent component analysis (ICA; Comon, 1994). This was initially proposed to provide a solution to the blind source separation (BSS) problem (Hérault, Jutten, & Ans, 1985), namely how to recover a set of unobserved sources mixed in an unknown manner from a set of observations. Since then, numerous algorithms based on the ICA concept have been employed successfully in various fields of multivariate data processing, from biomedical signal applications and communications to financial data modelling and text retrieval.

While linear mixtures of unknown sources have been examined thoroughly in the literature, the case of nonlinear ones remains an active field of research. This is due to the reduced representation of real-world datasets by the standard ICA formulation, which implies linear mixings of independent source signals. A common assumption of linear ICA-based methods is the absence of noise and that the number of mixtures must, at least, equal the number of sources.

Existing nonlinear ICA (NLICA) methods can be classified into two categories (Lee, 1999). The first models the nonlinear mixing as a linear process followed by a nonlinear transfer channel. These methods are of limited flexibility as they are often parametrized. On the other hand, the second category employs parameter-free methods, which are more useful in representing more generic nonlinearities. A common neural technique in this second category is the well known self-organizing map (SOM), mainly used for the modelling and extraction of underlying nonlinear data structures. SOMs (Kohonen, 1997) are neural network-based techniques using unsupervised learning and can provide useful data representations, such as clusters, prototypes or feature maps concerning the prototype (input) space. Early work on the application of SOMs to the NLICA problem has been done by Pajunen, Hyvärinen, and Karhunen (1996) and Herrmann and Yang (1996). Further work on NLICA has shown that there always exists at least one solution that is highly nonunique. However, additional constraints (e.g. the mixing function must be a conformal mapping from $\mathbb{R}^2$ to $\mathbb{R}^2$ and independent components must have bounded support densities) are needed to guarantee uniqueness (Hyvärinen & Pajunen, 1999).

The use of SOM-based separating structures can be justified as SOMs perform a nonlinear mapping from an input space to an output one usually represented as a low dimensional lattice. Using some suitable interpolation method (topological or geometrical), the map can be made continuous to provide estimates of the unknown signals.

* Corresponding author. Tel.: +44-161-200-4804; fax: +44-161-200-4784.

E-mail address: michelh@swift.ee.umist.ac.uk (M. Haritopoulos).

0893-6080/02/$ - see front matter
PII: S0893-6080(02)00081-3

However, there are difficulties associated with the nonlinear BSS (NLBSS) problem, such as its intrinsic indeterminacy and the unknown distribution of sources as well as the mixing conditions (which depend on the strength of the unknown nonlinear function involved in the mixing process), and the presence of noise (correlated or not). All these make it difficult for a complete analytical study of SOM behaviour when applied in this context.

The purpose of this paper is to show that an extended SOM-based technique can perform NLICA for the denoising of images. The advantages as well as the drawbacks of this technique, associated mainly with its high computational cost, will be discussed. After an overview of some signal denoising methods, followed by an introduction to the generic ICA problem and a brief presentation of some neural methods applied to the NLICA case, we will focus on the SOM's inherent nonlinear properties which make the NLBSS problem tractable. Then, we detail an image denoising scheme using SOMs. A comparative study between a modified SOM algorithm (Der, Balzuweit, & Herrmann, 1996), the original one and other nonlinear denoising techniques such as kernel principal component analysis (KPCA) and wavelet decomposition in the presence of multiplicative noise, will be validated by simulations and some real images.

2. Other signal denoising approaches

Image noise removal is traditionally achieved by linear processing techniques such as Wiener, low-, high- or band-pass filtering (Gonzalez & Woods, 2002). They can smooth (low-pass filters), enhance high spatial frequency characteristics (high-pass filters) or reduce specific noises (band-pass filters), while Wiener filtering is optimal in the least MSE sense. Their popularity is due to their mathematical simplicity and efficiency in the presence of additive Gaussian noise, but they tend to blur edges and do not remove heavy tailed (salt and pepper type noise, for example) and signal dependent noise. A classical nonlinear alternative to the above-mentioned drawbacks is median filtering defined as the median of all pixels within a neighbourhood of an image. It performs well in speckle noise removal and it preserves edge sharpness. An illustration example of its performance on real image data will be given for comparison purposes in Section 6.

Two other approaches providing promising results in the signal and the image denoising research areas are the KPCA and the wavelet transform. The former can be considered as a nonlinear generalization of linear principal component analysis (PCA). An introduction to KPCA with examples of its potential applications have been given by Müller, Mika, Rätsch, Tsuda, and Schölkopf (2001) and Schölkopf et al. (1999). The basic idea behind the kernel-based methods is the use of a kernel function k instead of dot products of the input space points, in order to map the data with a nonlinear mapping Φ associated with k, from the input space $\mathbb{R}^n$ to the feature space $\mathbb{F}$:

$$k(x, y) = (\Phi(x) \cdot \Phi(y)), \qquad x, y \in \mathbb{R}^n. \tag{1}$$

Kernels may be polynomial, sigmoid or radial basis functions (RBF) $k(x, y) = \exp(-\|x - y\|^2/c)$, to name but a few. Due to the kernel function (also known as the *kernel trick*), the mapping Φ does not need be explicit. Moreover, nonlinear problems in input space are transformed to linear ones in feature space, but, due to the nonlinear nature of the map Φ, not all points in $\mathbb{F}$ have exact pre-images in the input space. Mika et al. (1999) and Schölkopf, Mika, Smola, Rätsch, and Müller (1998) proposed an algorithm for computing approximate pre-images using kernels with the property $k(x, x) = 1$, $\forall x \in \mathbb{R}^n$, such as RBF functions, and applied it successfully to the denoising of 2D signals and images of handwritten digits. This kernel-based approach is linked with other nonlinear component analysis methods (Schölkopf, Smola, & Müller, 1999) and has been recently extended and applied to the NLBSS problem (Harmeling, Ziehe, Kawanabe, Blankertz, & Müller, 2001). It will be used for a comparison in Section 6.

Wavelet decomposition is based in the notion of optimal time–frequency localization (Mallat, 1989). Various wavelet transform-based techniques for signal and image denoising have been developed through the last decade. Probabilistic approaches model the wavelet coefficients associated with noise by various distributions and lead to signal-image enhancement by classical or optimal thresholding of these coefficients. Wavelet shrinkage has also been successfully used for image denoising (Donoho, Laird, & Rubin, 1995). It consists of nonlinearly transforming the wavelet coefficients by using fixed (standard wavelet shrinkage; Weyrich & Warhola, 1998) or adaptive (sparse wavelet shrinkage; Hoyer, 1999) transforms, reducing or suppressing thus low-amplitude values. Denoising by standard wavelet decomposition will be compared with our method in this paper.

3. Independent component analysis

The BSS problem was first introduced by Hérault et al. (1985), while the underlying ICA technique was first rigorously developed by Comon (1994) as a generalization of the PCA technique. ICA is one method for performing BSS that aims to recover unknown source signals from a set of their observations, in which they are mixed in an unknown manner. By minimizing the mutual information between the components of the output vectors of the demixing system, ICA tries to estimate *both* the mixing function and a coordinate system in which the source signal estimates become as mutually statistically independent as possible. A study of the stability, convergence and equivalent properties between various information-based

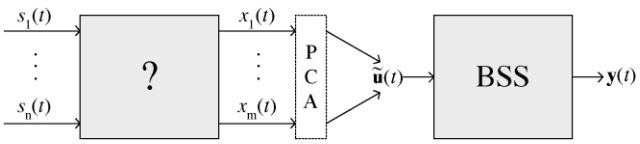

Fig. 1. General BSS mixing and separating structure.

techniques for ICA is given by Lee, Girolami, Bell, and Sejnowski (2000).

Let $\mathbf{x}(t) = [x_1(t), \ldots, x_m(t)]^{\mathrm{T}} \in \mathscr{X}$ be an m-dimensional mixture vector from the observation space and $\mathbf{s}(t) = [s_1(t), \ldots, s_n(t)]^{\mathrm{T}} \in \mathscr{S}$ the unknown n-dimensional source vector from the source space at discrete time t, where the superscript T denotes the matrix transpose operation. Then, the generic ICA problem can be formulated as

$$\mathbf{x}(t) = \mathscr{F}[\mathbf{s}(t)], \tag{2}$$

where $\mathscr{F}$ is the unknown and generally nonlinear transformation of the source vector. If $\mathscr{F}$ is linear, then some assumptions are necessary in order to estimate its inverse.

3.1. Linear ICA model

The most common linear ICA model is the *noiseless* one:

$$\mathbf{x}(t) = A\mathbf{s}(t), \tag{3}$$

where A is a $m \times n$ matrix, called the mixing matrix. The mutual statistical independence of the source components at a certain order and at each time index t is the basic assumption on which ICA is based to solve the BSS problem:

$$p[\mathbf{s}(t)] = \prod_{i=1}^{n} p[s_i(t)]. \tag{4}$$

Other common assumptions include that there are at least as many sensor responses as source signals, i.e. $m \geq n$ and that at most one Gaussian source is allowed. A study of all the necessary assumptions satisfying the strict mathematical conditions imposed by the ICA theoretical frame and grouped under the term 'separability' is given by Cao and Liu (1996).

3.1.1. Linear ICA and additive noise

Another concern is the presence of (generally) additive noise, which is usually assumed to follow a normal distribution. Denoting the additive noise vector by $\nu(t) = [\nu_1(t), \ldots, \nu_m(t)]^{\mathrm{T}}$ which will be called *sensor* noise in this article, then a more realistic and general ICA model is the *noisy* case:

$$\mathbf{x}(t) = A\mathbf{s}(t) + \nu(t). \tag{5}$$

Note, that the performance of many linear ICA algorithms depends on the mixing condition and that one can perform a signal noise separation by considering the noise (not the sensor noise) as a process with mutually independent components and independent from the source signal vector components and identify it as one of the source signals.

3.1.2. Pre-processing, source estimation and indeterminacies

A common pre-processing step in ICA-based techniques is 'whitening', also known as 'sphering' of the mixing vector $\mathbf{x}(t)$, to provide uncorrelated components $\mathbf{u}(t) = U(t)\mathbf{x}(t)$. The whitening matrix U is usually computed after singular- or eigen-value decomposition of the covariance matrix of $\mathbf{x}(t)$. After sphering, it is sufficient to estimate the orthogonal demixing matrix. The whitening can be performed by various techniques such as factor analysis (FA; Ikeda & Toyama, 2000) or linear PCA which yields zero mean and unit covariance (whitened) data, and so reduces the complexity of the linear BSS problem (Hyvärinen, 1999; Hyvärinen & Oja, 2000). Fig. 1 summarizes the mixing and separation steps in the general BSS problem.

Finally, if the noiseless ICA model of Eq. (3) is considered then ICA aims to find an estimated source signal vector $\mathbf{y}(t) = \hat{\mathbf{s}}(t)$ such that:

$$\mathbf{y}(t) = W\mathbf{x}(t) = WA\mathbf{s}(t). \tag{6}$$

W is the inverse linear transformation of A such that the components of the demixing system output vector $\mathbf{y}(t)$ are as independent as possible by maximizing objective (*contrast*) functions (Comon, 1994) according to certain criteria, such as the information maximization principle Infomax (Bell & Sejnowski, 1995). Note that, as defined in this section, W is optimal for the model of Eq. (3) but not for the noisy linear ICA model of Eq. (5). There still remains some indeterminacies intrinsic to the general linear BSS problem concerning the permutation, scale and sign of the estimated sources.

3.2. Nonlinear ICA model

Let us now consider the general ICA model (2) where $\mathscr{F}$ is a nonlinear transformation. In NLICA, the aim is to find a nonlinear transformation g so that the components of $\mathbf{y}(t) = g[\mathbf{x}(t)]$ are independent. NLICA applied to the NLBSS problem aims to find the inverse nonlinear transformation $\mathscr{F}^{-1}$ so that the source signals estimates vector $\mathbf{y}(t)$ satisfies:

$$\mathbf{y}(t) = \mathscr{F}^{-1}[\mathbf{x}(t)]. \tag{7}$$

In real problems it is more likely for $\mathscr{F}$ to be nonlinear and there is often a noise term to perturb the previous noiseless model. This noise term $\nu(t)$ can be additive or multiplicative, and with various distributions (correlated or not with the source signals). The complexity of the noisy NLICA model suggests the use of a flexible method that may need to be tailored to the experimental context. Except for the two general classes of NLICA methods introduced in Section 1, some research has addressed a compromise

between standard linear and purely NLICA methods, such as the ICA mixture models introduced by Lee, Lewicki, and Sejnowski (1999) and the local linear ICA using K-means clustering presented by Karhunen and Malaroiu (1999). The first tries to relax the independence assumption of the generic ICA model. While the second is closely related to the batch version of the SOM, but standard K-means clustering is used, because of the fairly small number of clusters involved.

Various artificial neural networks have also been applied to the NLBSS problem. The use of multilayer perceptrons (MLP) motivated by biomedical applications has been studied by Lee, Koehler, and Orglmeister (1997), while earlier Burel (1992) employed a two-layer perceptron. Recently, a RBF network (Tan, Wang, & Zurada, 2001) has been used to recover the unknown sources from their nonlinear mixtures in the presence of cross-nonlinearities. This method appears robust against additive, uniformly distributed white noise, but a further noise suppression technique is necessary to denoise the separated source signals. SOMs have been used by Pajunen et al. (1996) and Herrmann and Yang (1996) to extract independent components from nonlinearly mixed discrete or continuous sources. The network complexity increases with the number of neurons while the quantization error (interpolation error, in the continuous case) cannot be disregarded. Finally, a special form of nonlinear mixing, *post-nonlinear* mixing, was independently proposed by Taleb and Jutten (1997, 1999) and Lee et al. (1997). In this case, the sources are assumed to be linearly mixed and then transformed by a nonlinear transfer channel. This parametric approach uses sigmoidal functions and MLP networks to approximate the inverse nonlinearity. However, the approach is limited to a certain class of nonlinear mixtures and can be considered as fairly restrictive. A generalization to a rather larger class of functions is given by Hyvärinen and Pajunen (1999) using the notion of conformal mapping into the complex domain. We will now focus into the application of a SOM-based NLICA technique to the image denoising problem, after a brief revision of the SOM algorithm.

4. The SOM algorithm

The SOM algorithm is based on competitive learning and transforms an input space of arbitrary dimension using a topology preserving nonlinear mapping. Each neuron, j, $1 \leq j \leq l$ is connected to the input through a synaptic weight vector $\mathbf{w}_j = [w_{j1}, \ldots, w_{jm}]^{\mathrm{T}}$. At each iteration, SOM finds the best-matching (winning) neuron $\mathbf{v}$ by minimizing the following cost function:

$$\mathbf{v}(\mathbf{x}) = \arg\min_j \|\mathbf{x}(t) - \mathbf{w}_j\|, \qquad j = 1, \ldots, l, \tag{8}$$

where $\mathbf{x}$ belongs to an m-dimensional input space, $\|\cdot\|$ denotes the Euclidean distance, while the update of the synaptic weight vectors follows:

$$\mathbf{w}_j(t+1) = \mathbf{w}_j(t) + \alpha(t) h_{j,\mathbf{v}(\mathbf{x})}(t)[\mathbf{x}(t) - \mathbf{w}_j(t)], \quad j = 1, \ldots, l, \tag{9}$$

where $\alpha(t)$ and $h_{j,\mathbf{v}(\mathbf{x})}(t)$ designate the learning rate and the neighbourhood function centred on the winner, respectively. Although the algorithm is simple, its convergence and accuracy depend on the selection of the neighbourhood function, the topology of the output space, a scheme for decreasing the learning rate parameter, and the total number of neuronal units. For the experiments described below, we used the rules proposed by Haykin (1997) for the dynamic update of α and $h_{j,\mathbf{v}(\mathbf{x})}$.

4.1. Continuous SOMs

When dealing with continuous signals, an interpolation between the winner and its neighbours is necessary to make the map continuous. Different interpolation types can be employed. Geometric interpolation (Göppert & Rosenstiel, 1993) uses orthogonal projections, in the n-dimensional SOM's output layer, of the vector formed by the approximation to the exact input onto the one formed by the approximation of the second best-matching unit. Topological interpolation (Göppert and Rosenstiel, 1995) is based on selecting the topological neighbours of the winner, which is an advantage over the geometrical method unless there are topological defects on the chosen map.

4.2. SOM in presence of noise

A modified version of the original Kohonen algorithm for constructing nonlinear data models in the presence of noise is given by Der et al. (1996), which provides a good approximation of the principal manifolds modelling the data distributions in the presence of multiplicative noise. The novel aspect of this algorithmic scheme is the use of an individual neighbourhood for each neuron. The width of the Gaussian neighbourhood functions is adjusted to keep them near their critical value. By averaging over the deviations of the input samples from the winning neurons, an estimate of the manifold in the data space can be obtained. In Section 6, we show that this modified algorithm outperforms the original SOM when applied to simulated signals as well as to test images.

4.3. NLICA using SOMs

The initial results on the application of SOMs to the NLBSS problem were reported by Pajunen et al. (1996). Finding an inverse nonlinear transform $\mathscr{F}^{-1}$ from $\mathbb{R}^n \rightarrow \mathbb{R}^n$ is not a trivial problem unless additional constraints are applied. Here, the authors restricted $\mathscr{F}$ to the family of *homeomorphism* functions. The desired mapping must be

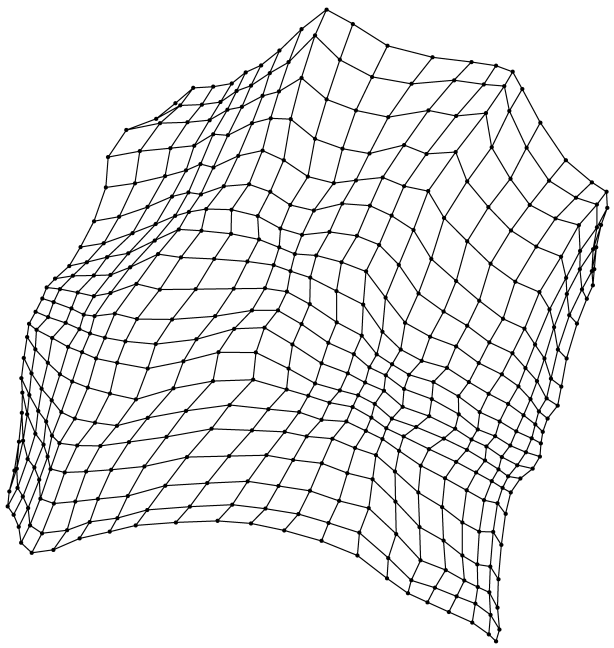

Fig. 2. Example of a converged 2D Kohonen map.

topology-preserving, a property which is satisfied if the two best-matching units of the SOM are connected neighbours. Definition of topographic functions and a generalization of the topology preservation property for more general lattice structures are given by Villmann, Der, Herrmann, and Martinetz (1997). However, restrictions apply to this approach. The mixing model is assumed to be linear, which is then nonlinearly distorted. The further the source probability density functions (pdf) are from a uniform one or the stronger the nonlinearities involved in the mixing process, the more difficult it is to impose a rigorous mapping of the input data to the nodes of the map. However, for mildly nonlinearly mixed, sub-Gaussian source signals and for a rectangular output lattice, it can been shown, at least heuristically, that the SOM provides a rough approximation of the unknown sources (Karhunen, 2001). An example of a converged SOM map on a 2D observation vector made up with mildly nonlinearly mixed signals is shown in Fig. 2. Finally, extension of the previous work by Herrmann and Yang (1996) has shown that SOMs can be used to solve the NLBSS problem under some constraints.

The SOM constitutes a parameter-free approach to the NLBSS problem as it can provide a solution due to its inherent property of performing nonlinear projections from a high dimensional data manifold into a low dimensional grid. The main drawback remains its high computational cost as the network complexity increases with the number of neurons and with the quantization error (interpolation error in the continuous case; Yang, Amari, & Cichocki, 1997). On the other hand, the approach is robust and can be very easily adapted within the NLICA framework. Indeed, applying SOMs to this context is straightforward, if one matches the ICA observation space $\mathscr{X}$ and source space $\mathscr{S}$ to the SOM input layer and output layer, respectively. It then remains to define the model vectors $\mathbf{w}_j$, $1 \leq j \leq l$ and perform an appropriate interpolation step to complete the separation task, if continuous sources are desired.

5. A SOM-based signal denoising method

Many data processing applications concern the removal of noise and most BSS research using ICA techniques concerns specific noise distributions (usually additive noise) or is based on the low amplitude/noiseless model as described by Eq. (3). However, real world signals are often corrupted in a more complex way. The signal-to-noise ratio (SNR) of all low light level images is dominated by photon, or shot, noise due the random arrival of individual photons at a detector. This noise source is multiplicative in nature. Other noise sources include speckle, salt and pepper or quantization noise occurring in an additive or multiplicative manner and which can be fitted to various distributions such as Gaussian or Poisson. Such factors cause many existing NLICA techniques to fail. As SOMs offer a data-driven, parameter-free, nonlinear approximation method, one can consider a SOM-based NLICA technique as an alternative to other techniques such as sparse code and wavelet shrinkage, mentioned earlier.

5.1. Image denoising using a 2D SOM

The proposed image denoising method requires at least two image frames of the same scene and does not use any additional information concerning either the sources or the mixtures. The pre-processing of the images set as well as the post-processing step dealing with the indeterminacies inherent to the ICA problem are presented and discussed.

5.1.1. Pre-processing of the image data

Each one of the two available image frames I of dimension $d_h \times d_w$ pixels (height × width) is decomposed into distinct windows of dimension $p = N_h \times N_w$ pixels. Hence, one obtains $N = (d_h/N_h) \times (d_w/N_w)$ sub-images I_j, $1 \leq j \leq N$ rearranged as 1D vectors of length p and normalized. Finally, the sub-images are whitened by standard PCA. From now on, we will denote by I_{1j} and I_{2j}, $1 \leq j \leq N$ the sub-images corresponding to the first and the second available image frames, respectively.

5.1.2. Definition of the sources and the mixtures

Applying a SOM-based NLICA technique requires the determination of the sources, mixtures and verification of the separability property (Section 3.1). The last is a very difficult task within a nonlinear framework. Nevertheless, it is reasonable to assume that the sources to be separated are a denoised version of the original image frames and the noise contained in those images. For this to be valid, the output of the SOM must be a 2D lattice that recovers the two

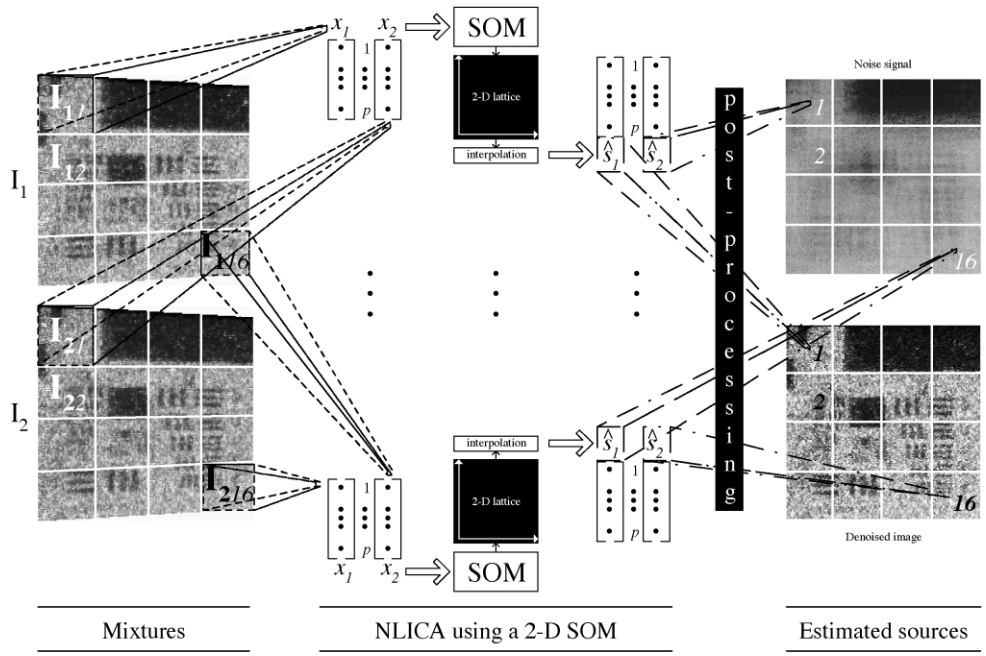

Fig. 3. Image pre-processing and SOM-based source separation.

separated sources $\mathbf{y}(t) = [\hat{s}_1(t), \hat{s}_2(t)]$ corresponding to the denoised sub-image and the noise, respectively. As for the mixture vector $\mathbf{x}$, it is composed by the sub-images I_{1j} and I_{2j} $1 \leq j \leq N$ generated in the pre-processing step. Fig. 3 shows the employed two mixtures–two sources approach. After SOM convergence and interpolation of its output coordinates, it remains to rearrange and reposition the estimated vectors with respect to the whole image frame to obtain a normalized version of the partially reconstructed denoised image and noise signals. Repeating this process for all the N sub-images I_{1j} and I_{2j}, leads to the estimation of two signals: (i) an enhanced version of the noisy image frame and, (ii) a noise which corrupted both image frames.

5.1.3. Relaxing the indeterminacies

The main indeterminacies arising from the proposed separation scheme concern the order and sign of the separated signals. As the whole image I is windowed, there is no guarantee that the entire set of the estimated sub-images $\hat{s}_1$ and $\hat{s}_2$ will be of the same scale and sign (note that, the scale indeterminacy does not affect the denoising scheme). This is more problematic when the image is too large and p is chosen too small, unless a reliable technique is found to rearrange automatically the separated signals. The order of the estimated signals for each sub-image may not necessarily remain unchanged. It is not certain that each one of the first and the second ith and jth, $1 \leq i, j \leq N$ estimated sub-images belongs to the first and the second global reconstructed images, respectively. This means that a classification procedure after separation is needed.

In order to overcome these problems, we implemented a method based on the correlation coefficient ρ which for two random variables X_i and X_j is defined as $\rho_{i,j} = C_{ij}/\sqrt{C_{ii}C_{jj}}$), where C_{ij} is the covariance of X_i and X_j and $\rho_{i,j} \in [-1, 1]$, which vanishes for independent variables. First, according to

$$\bar{\rho}_{i,j} = \tfrac{1}{2}(\rho_{I_{1j},\hat{s}_{ij}} + \rho_{I_{2j},\hat{s}_{ij}}), \qquad \forall j \in [1, N], i = 1, 2, \tag{10}$$

the order of the separated sub-images will be switched whenever the condition $|\bar{\rho}_{1,j}| < |\bar{\rho}_{2,j}|$, $1 \leq j \leq N$ is satisfied. After the classification procedure, the sign of each estimated and normalized sub-image vector will be inverted depending on:

$$\bar{\rho}_{i,j} < 0, \qquad \forall j \in [1, N], i = 1, 2. \tag{11}$$

This automated task of *classification* and *sign inversion* has proven to be robust, but only the first step is essential as the experimental results will confirm.

5.1.4. Post-processing and multiplicative noise removal

As mentioned in Section 4.3, divergence of the true sources pdf from the uniform one or strong nonlinearities may result in poor separation results by a SOM network. Furthermore, it is assumed that we have no prior knowledge about the way the noise source corrupted the images. For these reasons, and because the raw separated images issued from experiments with test and real image frames are still correlated with the noise source, we now describe the proposed image enhancement method.

Let us consider the following NLICA model for the two mixtures–two sources case:

$$x_1(t) = s_1(t)[1 + \alpha_1 s_2(t)], \qquad x_2(t) = s_1(t)[1 + \alpha_2 s_2(t)], \tag{12}$$

where s_1 and s_2 correspond to the noise-free image and the noise source, respectively. Some remarks can be made about

Table 1
SNR (in dB) for NLICA with SOM and SOM-m algorithms

		SOM	SOM-m	SOM (with PCA)	SOM-m (with PCA)
$\sigma^2 = 0.01$	$\hat{s}_1$	5.72	3.36	3.36	4.72
	$\hat{s}_2$	7.7	7.53	8.16	8.36
$\sigma^2 = 0.1$	$\hat{s}_1$	1.94	4.11	2.85	4.31
	$\hat{s}_2$	6.09	6.61	7.21	6.67

this model. First, it assumes that the noise component s_2 is common to both sources and that only its contribution varies from frame to frame. Moreover, one could complete the previous model by a noise term ν corresponding to the sensor noise (see Section 3.1.1) which can be additive (e.g. thermal noise, quantization noise), multiplicative (e.g. speckle) or which can corrupt the image in a more complex way. In the absence of any prior knowledge concerning the noise, we considered the simplified model of Eq. (12) that we validated by experiments on test and real images.

After convergence of the SOM network and assuming that the SOM approximated well the inverse nonlinear transformation, we obtain the estimated noise-free image $\hat{s}_1$. But, experiments have shown that some sub-image parts of $\hat{s}_1$ still remain noisy after separation. So, we enhance each one of the noisy frames by adding (subtracting) a slightly increasing quantity $\alpha = \{\alpha_1, \alpha_2\}$ of the normalized estimated noise source $\hat{s}_2$ to (from) the available noisy image frames. This can be formulated by:

$$\begin{aligned} \hat{s}_{11}(t) &= x_1(t)[1 \pm \alpha_1 \hat{s}_2(t)]^{-1}, \\ \hat{s}_{12}(t) &= x_2(t)[1 \pm \alpha_2 \hat{s}_2(t)]^{-1}, \end{aligned} \tag{13}$$

where $\hat{s}_{11}$ and $\hat{s}_{12}$ are enhanced versions of the first and the second noisy frames, respectively. A unique denoised image may be obtained by averaging over $\hat{s}_{11}$ and $\hat{s}_{12}$. The coefficients α_{opt} are optimal in the peak signal-to-noise ratio (PSNR) sense, defined as:

$$\text{PSNR} = 10 \log_{10}\left(\frac{p_{\max}^2}{\text{MSE}}\right), \tag{14}$$

where $p_{\max}$ is the maximum value of the image pixel intensity and MSE denotes the mean-squared error between the original image and its estimate. However, this requires additional knowledge concerning the noise-free image (Hoyer, 1999). For real image denoising, α_{opt} is determined empirically.

6. Experiments

In this section, we first compare the performances of the SOM algorithm and its modified version on simulated nonlinear mixtures as well as test images. Then we apply the previously described SOM-based image denoising scheme to real images, together with a performance analysis of the proposed approach. Note also that for all of our experiments we used greyscale images.

6.1. Simulation on continuous sources

In order to compare the performances of the original SOM algorithm (Section 4) and its modified version (Section 4.2), which will be denoted by SOM-m, we carried out simulations using the same signal sources as given by Pajunen et al. (1996). The first source s_1 is a sinusoid and the second source s_2 a uniformly distributed white noise. These sub-Gaussian signals were first mixed linearly with matrix

$$A = \begin{bmatrix} 0.7 & 0.3 \\ 0.3 & 0.7 \end{bmatrix},$$

whose determinant has a value of 0.4 ensuring the well conditioning of the mixing, providing thus the observation vector $\mathbf{x}$ ($m = 2$). This vector was next transformed nonlinearly by using:

$$\mathscr{F}(\mathbf{x}) = \mathbf{x}^3 + \mathbf{x}. \tag{15}$$

Clearly, the observations are obtained as post-nonlinear mixtures of the sources: $\mathbf{x} = \mathscr{F}(A\mathbf{s})$ (Taleb & Jutten, 1999). Finally, they were corrupted with multiplicative noise ν of arbitrary variance σ^2, generated randomly from a uniform distribution.

Table 1 summarizes the results of this simulation, where $\hat{s}_1$, $\hat{s}_2$ denote the sinusoid and the white noise sources and their estimates, respectively. Some experiments also employed a PCA pre-processing before applying the SOM-based NLBSS method and used the SNR to quantify the separation results.

For the source of interest being s_1, it can be observed that in the absence of a pre-whitening step and excepting the case of small noise variance ($\sigma^2 = 0.01$), SOM-m greatly enhances the SNR. While, when applying a PCA pre-treatment to the mixtures, the locally varying neighbourhood width of the SOM-m algorithm in conjunction with the presence of noise helps the map during training to escape from local minima. Nevertheless, due to the correlation of the noise with each of the source signals, the estimated sources remain fairly noisy, as illustrated in Fig. 4. In summary, the SOM-m algorithm performs better than the standard SOM (with and without pre-whitening) in presence of multiplicative noise.

An overall image of the performance of linear and nonlinear techniques, is provided by Table 2 which shows comparative results between linear PCA and ICA, the SOM-m algorithm and denoising by wavelet coefficients thresholding (using the Daubechies decomposition). The previously described mixture vector $\mathbf{x}$ is used for the simulations, but this time are tested for linear (L) and nonlinear (NL) models constructed under Eq. (15) and corrupted by additive (A) as well as multiplicative (M) noise of arbitrary variance.

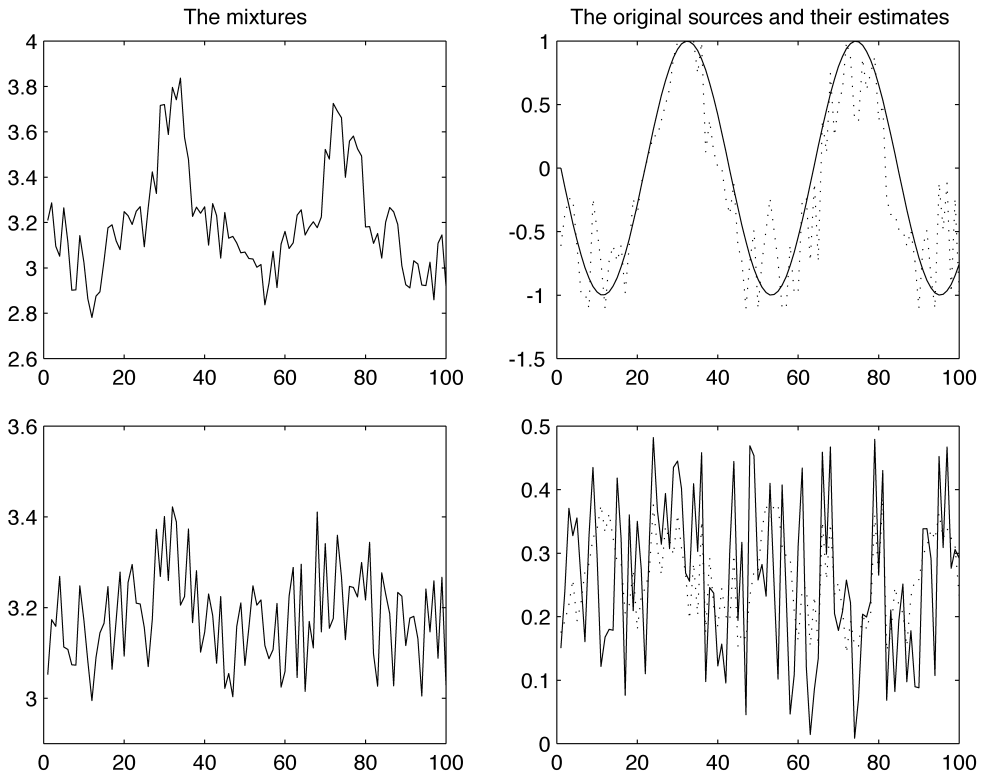

Fig. 4. The observations (left column) and the estimated sources (dotted) obtained by SOM-m in presence of multiplicative noise together with the original ones (right column).

In the NL case, linear methods like PCA and ICA (the JADE algorithm (Cardoso & Souloumiac, 1993)) perform poorly; the SNR is relatively close to the one provided by SOM-m, but clearly, the estimated signal $\hat{s}_1$ is very different from the original one. The same is valid for the wavelets method applied to denoise one of the nonlinear mixtures, which leads to signals with very smooth waveforms containing sharp peaks, increasing thus the SNR. On the contrary, estimation of the useful signal from linear mixtures improves the SNR for all the proposed methods, while the best results are provided by the JADE algorithm. These results confirm that nonlinear methods like SOM-based algorithms can be very useful in signal estimation and denoising.

Table 2
SNR (in dB) for the estimated sinusoid by linear and nonlinear methods applied to linear (L) and nonlinear (NL) mixture models corrupted by additive (A) and multiplicative (M) noise of variance σ^2

Model	σ^2	SOM-m (with PCA)	Linear ICA	Linear PCA	Wavelets
L + A	0.01	10.29	14.45	9.63	9.34
L + A	0.1	10.44	12.69	9.33	8.39
NL + M	0.01	4.72	3.51	4.02	5.73
NL + M	0.1	4.31	3.94	2.89	4.77
L + M	0.01	6.35	14.44	9.64	13.49
L + M	0.1	9.37	13.1	9.53	13.24
NL + A	0.01	4.11	3.38	4.06	5.81
NL + A	0.1	2.91	2.92	3.83	5.49

6.2. Image denoising and comparison

Our first image set is a 50×100 pixel region of the Lena image, containing representative features with high contrast and which constituted the first source. The second one is a uniformly distributed random noise of zero mean and arbitrary variance. These two sources, supposed unknown, were mixed in a multiplicative manner, using noise variances of 0.05 and 0.01 to form the observations consisting of two noisy versions of the Lena image. The mixing was constructed according Eq. (12) with $\alpha_1 = \alpha_2 = 1$.

A $N_h \times N_w$ pixels size windowing is used to decompose each noisy image into an N dimensional vector containing p samples each (see Section 5.1.1 for notations). To each one of the sub-images I_{1j} and I_{2j}, $1 \leq j \leq N$ of the whitened 2D observation vector we apply the SOM-based separation scheme. Thus, we obtain the estimated source vector y whose components $\hat{s}_1(t)$ and $\hat{s}_2(t)$ correspond to the denoised image and the noise source, respectively, after the classification and sign inversion steps (Section 5.1.3) and the noise removal procedure (Section 5.1.4).

As the original SOM algorithm does not cope with the multiplicative noise as well as its modified version SOM-m, we present here the denoising results obtained using the latter. Fig. 5 shows the original image and the two separated signals after interpolation and before removing the indeterminacies. They were computed by the SOM-m based

(a) (b) (c)

Fig. 5. Original Lena image (a) and the separated denoised version (b) and noise (c).

NLBSS approach using a 18×18 neuronal map. The windowing size is $N_h = N_w = 10$ pixels. The above choice for the number of neuronal units provides a fine granularity of the map and good precision after interpolation of the discrete nodes coordinates. After classification and noise removal, two denoised versions $\hat{s}_{11}$ and $\hat{s}_{12}$ of the Lena image are obtained as shown in Fig. 6. The more noisy mixture (a) is enhanced in terms of PSNR by 1.6 dB (b), while from the second noisy frame (c), an improved by 0.5 dB version (d) is deduced. Note that linear ICA algorithms, such as JADE, are unable to provide independent sources as confirmed by the form of the joint distribution of the estimated sources in Fig. 7.

The classification task of Eq. (10) is illustrated by Fig. 8. The crosses denote the values of $\bar{\rho}_{i,j}$, $i = 1$, $\forall j = 1, \ldots, N$ which correspond to the separated image source and the circles represent $\bar{\rho}_{i,j}$, $i = 2$, $\forall j = 1, \ldots, N$ corresponding to the separated noise source signal, where $N = 50$. A correlation coefficient with an absolute value of 1 shows a linear dependence between the two variables: it is the case of $\hat{s}_1$ whose mean correlation coefficients (crosses) with the available sub-mixtures I_{1j} and I_{2j}, $j = 1, \ldots, N$ are concentrated near ± 1. So, if $|\bar{\rho}_{1,j}| < |\bar{\rho}_{2,j}|$, $1 \leq j \leq N$, the estimated sub-image will be part of the estimated image signal; in the opposite case, it will belong to the second estimated source, i.e. the noise signal. In this example, only three sub-images ($j = 25, 40, 48$ corresponding to the solid lines in Fig. 8) will have to be classified properly after the SOM-m projection.

After the classification step, there remains the sign indeterminacy to be solved before applying the proposed denoising rule. Eq. (11) for sign correction of the estimated image source $\hat{s}_1$ provides only a visual matching between the available image frames and their estimated denoised version. It cannot be used to adjust the sign of the estimated noise signal $\hat{s}_2$ as, at least theoretically, the recovered noise must be independent from the image source. As the proposed denoising scheme is based on the separated noise signal $\hat{s}_2$, by increasing the coefficients α in Eq. (13), some regions of interest in the denoised image become blurred, suggesting a problem with the sign of $\hat{s}_2$. In this case a manual adjustment is required.

We also performed experiments using approximate pre-image reconstruction via KPCA (Section 2) to the previous noisy image set. We used distinct windowing of 10 pixels size with kernel parameter c equalling twice the data's average variance in each dimension, as suggested by Mika et al. (1999). The images have been reconstructed using various numbers of principal components to compute the approximate pre-images. The KPCA performed poorly in these experiments. No enhancement of the PSNR ratio is noticed due to the experimental context, in which only two noisy frames constitute the image database available for training. For a visual inspection of the results provided by this method, Fig. 9 shows the denoised images after projection onto the first three principal components in feature space. To ensure that the proposed denoising scheme may be applied within the KPCA framework, we reconstructed denoised versions of the previous Lena image, this time contaminated by additive Gaussian noise of zero mean

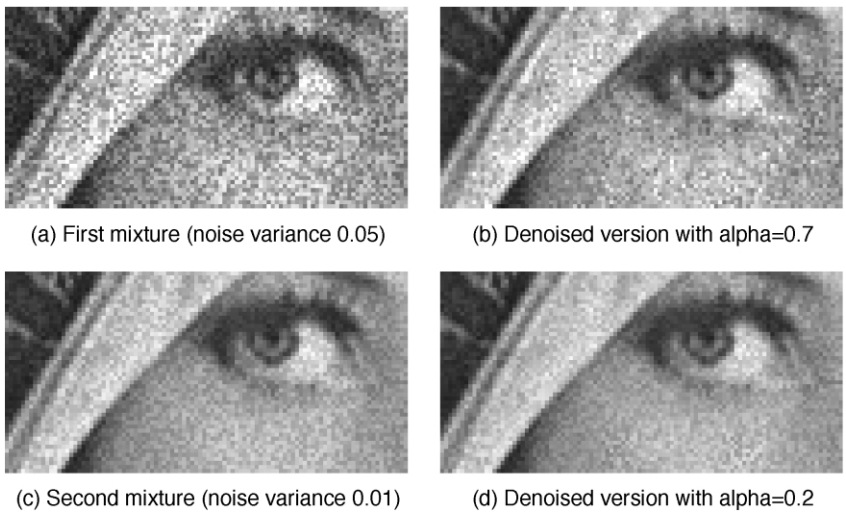

(a) First mixture (noise variance 0.05) (b) Denoised version with alpha=0.7

(c) Second mixture (noise variance 0.01) (d) Denoised version with alpha=0.2

Fig. 6. The noisy images (a and c) and their denoised versions (b and d) using the SOM-m algorithm.

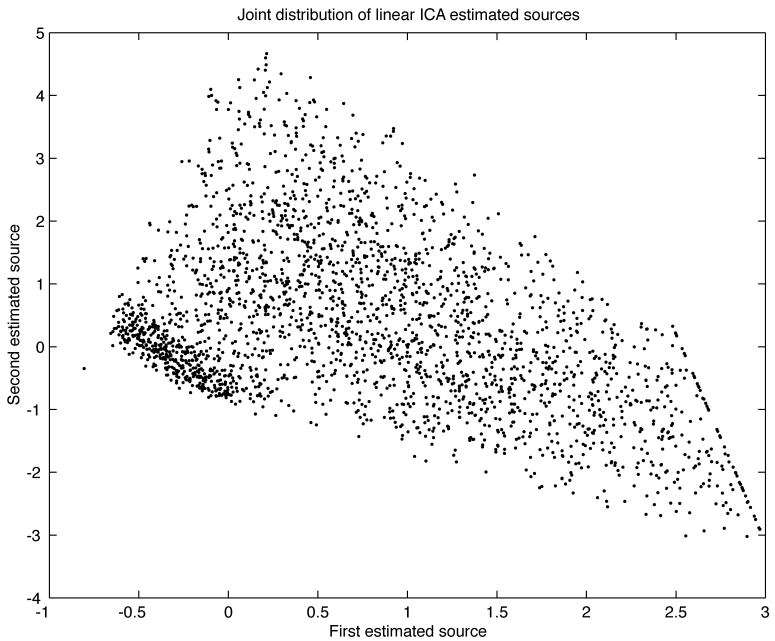

Fig. 7. Joint distribution of estimated sources using linear ICA.

and variance 0.05 and 0.01 to form the first and the second mixture, respectively. In this case, KPCA reconstruction by the approximate pre-images method, provided a slight enhancement in terms of PSNR, the importance of which depended on the number of principal components used for the projection in the feature space. We do not present further results concerning the additive noise case as it is beyond the paper's scope.

Finally, some experiments using MATLAB functions for wavelet decomposition (Daubechies) and denoising by hard thresholding and pixel-wise adaptive Wiener filtering based on local statistics (*wiener2*), provided an enhancement of 3.1 and 3.07 dB for the more noisy image and 1.1 and 2.28 dB for the second one in terms of PSNR, respectively. The resulting images are shown in Fig. 9. Despite the higher PSNR values, the results provided by both methods are very smooth and in small size images appear more blurred, while with our method, images keep their sharpness and edges practically unaffected.

Another experiment was undertaken with the same image set but with a different windowing size ($N = 25$) and number of neurons (42×42). Application of our denoising

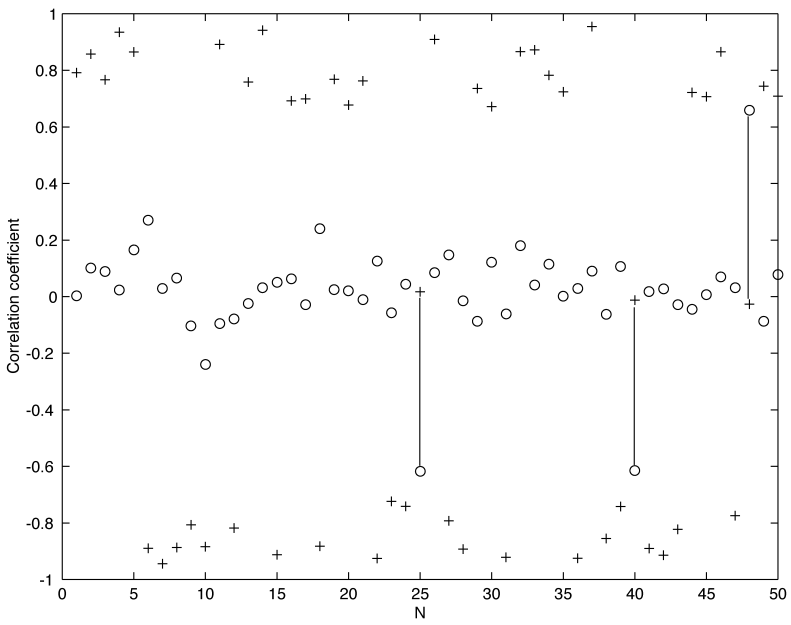

Fig. 8. Classification step of the SOM-separated image (crosses) and noise (circles) signals.

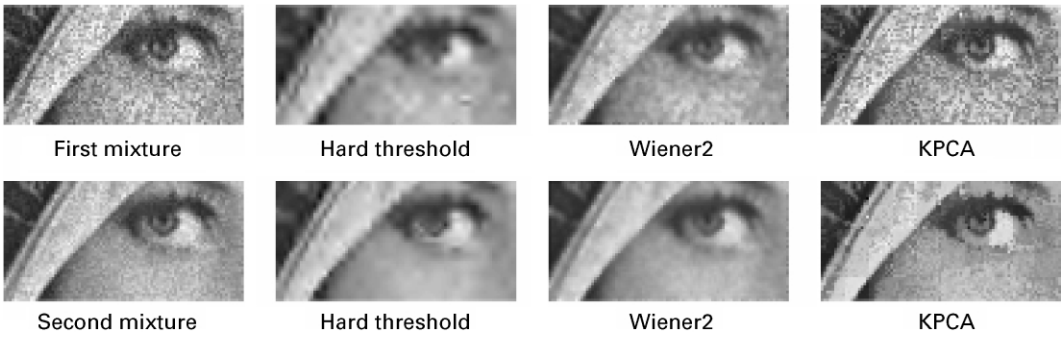

Fig. 9. Comparative denoising results.

method yielded an increase of the PSNR ratio of 2.32 dB for the more noisy frame and of 0.61 dB for the second one. This demonstrates the importance of the choice of N. This has also been noted by Hurri (1997). There are no specific rules for the choice of this parameter; it depends strongly on the type of images, the application and the windowing type (distinct or overlapping blocks).

The computation of the α_{opt} parameter by which the PSNR is maximized (Section 5.1.4) is achieved by making α vary in the denoising rule, Eq. (13), over a certain range, e.g. [0,1.5] and, with constant steps, that leads to the results of Fig. 10. The PSNR for the denoised versions of the more (dashed line) and less (solid line) noisy image frames is maximized for an optimum alpha of 0.69 and 0.19, respectively. The interesting evolution curves of this performance measure, which constitutes the PSNR (Eq. (14)), are similar to those matching an aperiodic stochastic resonance (ASR) effect (Collins, Chow, Capela, & Imhoff, 1996). The latter characterizes nonlinear systems and can be defined as a noise-assisted signal enhancement method (Godivier, 1993).

Next, the proposed method is applied to denoise noisy infrared vision images. A total of 24 consecutive frames were taken, containing a test pattern of numerals as well as horizontal and vertical bars. In this experiment, we used two nonconsecutive image frames as mixtures, as shown in Fig. 11.

The images of size 200×200 pixels are first pre-processed by standard PCA with a windowing size of 50×50 pixels. By applying a linear PCA, or ICA, to these signals, we obtain the estimated images (a) and (b) of Fig. 12. It is clear that the separated signals are still correlated with the noise contained in the original frames. The raw separated signals provided by the standard SOM algorithm after interpolation of their co-ordinates are then classified, and their sign readjusted.

Denoising according to Eq. (13) does not provide satisfactory results. The first separated image is still correlated with the noise. However, using $\hat{s}_1$ instead of $\hat{s}_2$ in the previous equations and, finally, by averaging over the two obtained images $\hat{s}_{11}$ and $\hat{s}_{12}$, one obtains interesting results shown in Fig. 13(a). For a comparison, we applied a

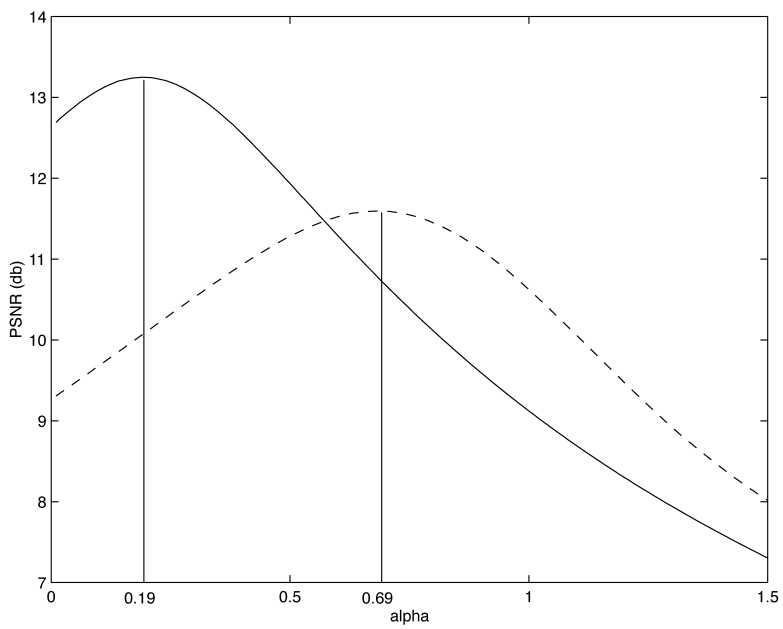

Fig. 10. PSNR evolution curves for both input signals in function of α.

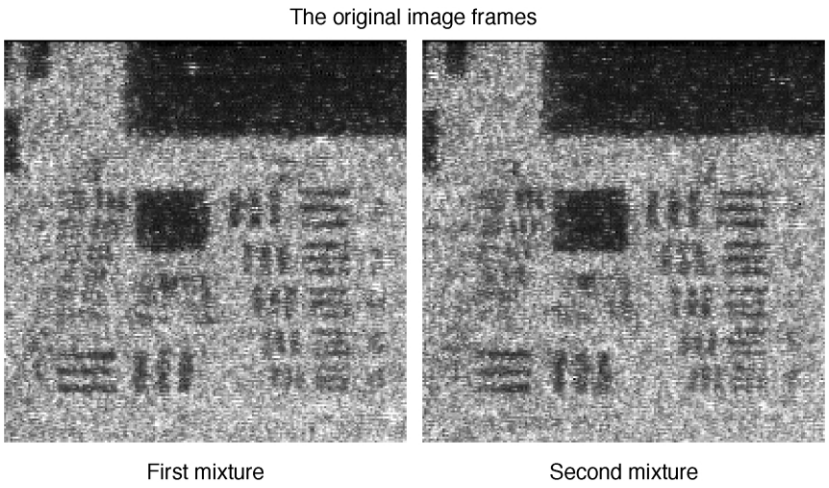

Fig. 11. The raw test image frames.

median filter to the histogram equalized mixtures, as shown in the right-hand side image (b). One can remark the lack of sharpness after median filtering while there is no information loss by the proposed method. Also, that the estimated image still contains noise helps this scheme to work as a signal enhancement method.

Finally, the SOM-based denoising technique is time consuming, especially when training large maps. The computational complexity of the SOM algorithm for one training step is $\mathcal{O}(ld)$ where l is the number of neurons and d is the dimensionality of the map. The complexity of one training epoch is $\mathcal{O}(pld)$ where p denotes the number of data samples, while the number of training epochs determines the complexity of the whole training. In our experiments, we wanted a fairly high granularity on the output map, in order to obtain a good precision on the source estimates after interpolation. The training is stopped when the variation of the network weights values over 1000 iterations is smaller than a fixed threshold. Note also that, in general, the choice of the number of map units is quite arbitrary and that the computational intensity of the SOM training task is also dependent on the memory demands. As there is no formal proof of the convergence of SOM in higher than 1D spaces, empirical methods are needed to determine its computational complexity.

7. Discussion

This work constitutes a first attempt towards a SOM-based image denoising and shows that a SOM-based NLICA method can be applied in this particular context. It is based on the nonlinear projection property inherent in SOM neural networks and offers an alternative solution to existing denoising schemes. Its main advantages are (i) that it performs in a completely blind context where there is no prior knowledge concerning the noise-free images and noise properties, and (ii) it can provide satisfactory results from only two noisy frames. Although SOMs behave well in denoising 1D and simulated noisy 2D signals, the interpretation of the results obtainable when naturally noisy images are involved is more complex and needs further investigation. However, the main restrictive aspect of this approach for real world image denoising applications

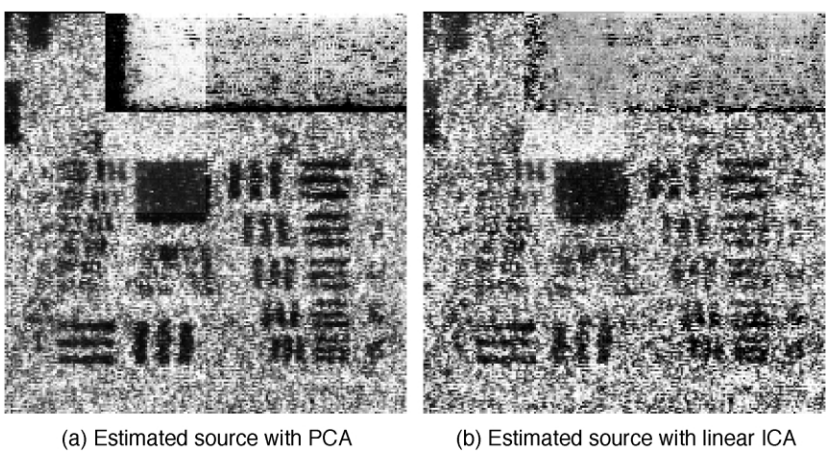

Fig. 12. Separated signals obtained by PCA (a) and linear ICA (b).

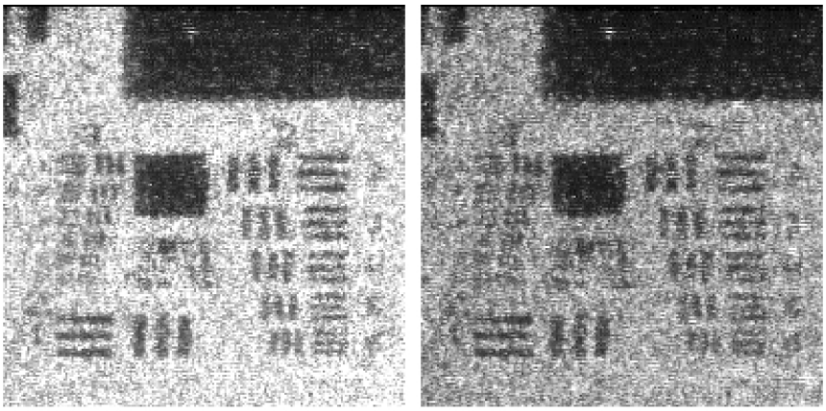

(a) Denoised image (b) Median filter

Fig. 13. Enhanced image (a) and best median filter (b).

is the computational cost, which grows exponentially with the dimensions of the output lattice. Our current work is focused on the characterization of the separated noise properties in this particular context. As it has been pointed out that there is no unique solution to the NLBSS problem, our research aims to determine a nonlinear model which with some limited restrictions, could lead to a more precise description of the mixing process.

Acknowledgments

This work is supported by UK EPSRC grant GR/R 01460.

References

Bell, A.-J., & Sejnowski, T.-J. (1995). An information-maximization approach to blind source separation and deconvolution. *Neural Computation*, *7*(6), 1129–1159.

Burel, G. (1992). Blind separation of sources: A nonlinear neural algorithm. *Neural Networks*, *5*, 937–947.

Cao, X.-R., & Liu, R. W. (1996). General approach to blind source separation. *IEEE Transactions on Signal Processing*, *44*, 562–571.

Cardoso, J.-F., & Souloumiac, A. (1993). Blind beamforming for non gaussian signals. *IEE Processings-F*, *140*(6), 362–370.

Collins, J. J., Chow, C.-C., Capela, A.-C., & Imhoff, T.-T. (1996). Aperiodic stochastic resonance. *Physical Review E*, *54*(5), 5575–5584.

Comon, P. (1994). Independent component analysis—A new concept? *Signal Processing*, *36*, 287–314. Special issue on Higher-Order Statistics.

Der, R., Balzuweit, G., & Herrmann, M. (1996). Building nonlinear data models with self-organizing maps. In C. van der Malsburg, W. von Seelen, J. C. Vorbruggen, & B. Sendhoff (Eds.), *Artificial neural networks* (pp. 821–826). Berlin: Springer.

Donoho, D. L., Laird, N., & Rubin, D. (1995). Wavelet shrinkage: Asymptopia? *Journal of the Royal Statistical Society, Series B*, *57*, 301–337.

Godivier, X. (1993). *La résonance stochastique dans la transmission non linéaire du signal*. Thèse de doctorat, LISA-Université d'Angers, available at http://www.geocities.com/SiliconValley/Platform/6421/resume/chgthese.htm.

Gonzalez, R. C., & Woods, R. E. (2002). *Digital image processing* (2nd ed.). Englewood Cliffs, NJ: Prentice-Hall.

Göppert, J., & Rosenstiel, W. (1993). Topology preserving interpolation in self-organizing maps. *Proceedings of NEURONIMES'93* (pp. 425–434).

Göppert, J., & Rosenstiel, W. (1995). Topological interpolation in SOM by affine transformations. *Proceedings of ESANN'95*.

Harmeling, S., Ziehe, A., Kawanabe, M., Blankertz, B., & Müller, K.-R. (2001). Nonlinear blind source separation using kernel feature spaces. *Proceedings of the Third International Conference on Independent Component Analysis and Signal Separation, ICA 2001*, San Diego, CA, USA, December 2001 (pp. 102–107).

Haykin, S. (1997). *Neural networks—A comprehensive foundation* (2nd ed.). New Jersey: Prentice-Hall.

Hérault, J., Jutten, C., & Ans, B. (1985). Détection de grandeurs primitives dans un message composite par une architecture de calcul neuromimétique en apprentissage non supervisé. *Proceedings of GRETSI'85* (pp. 1017–1020).

Herrmann, M., & Yang, H. H. (1996). Perspectives and limitations of self-organizing maps in blind separation of source signals. *Progress in Neural Information Processing: Proceedings of ICONIP'96* (pp. 1211–1216).

Hoyer, P. (1999). *Independent component analysis in image denoising*. M.S. thesis, Helsinki University of Technology, Espoo, April 1999, available at http://www.cis.hut.fi/~phoyer/papers/.

Hurri, J. (1997). *Independent component analysis of image data*. M.S. thesis, Helsinki University of Technology, Espoo, March 1997, available at http://www.cis.hut.fi/~/publications/.

Hyvärinen, A. (1999). Survey on independent component analysis. *Neural Computing Surveys*, *2*, 94–128.

Hyvärinen, A., & Oja, E. (2000). Independent component analysis: Algorithms and applications. *Neural Networks*, *132*(4–5), 411–430.

Hyvärinen, A., & Pajunen, P. (1999). Nonlinear independent component analysis: Existence and uniqueness results. *Neural Networks*, *12*(3), 429–439.

Ikeda, S., & Toyama, K. (2000). Independent component analysis for noisy data—MEG data analysis. *Neural Networks*, *13*, 1063–1074.

Karhunen, J. (2001). Nonlinear independent component analysis. In R. Everson, & S. Roberts (Eds.), *ICA: Principles and Practice* (pp. 113–134). Cambridge: Cambridge University Press.

Karhunen, J., & Malaroiu, S. (1999). Local independent component analysis using clustering. *Proceedings of the First International Workshop on Independent Component Analysis and Signal Separation, ICA'99*, Aussois, France, January 1999 (pp. 43–48).

Kohonen, T. (1997). *Self-organizing maps* (2nd ed.). *Springer series in information science no. 30*, Berlin: Springer.

Lee, T.-W. (1999). Nonlinear approaches to independent component analysis. *Proceedings of American Institute of Physics*.

Lee, T.-W., Girolami, M., Bell, A.-J., & Sejnowski, T.-J. (2000). A unifying information—Theoretic framework for independent component analysis. *Computers and Mathematics with Applications*, *31*(11), 1–21.

Lee, T.-W., Koehler, B.-U., & Orglmeister, R. (1997). Blind source separation of nonlinear mixing models. In J. Principe, L. Gile, N. Morgan, & E. Wilson (Eds.), *Proceedings of 1997 IEEE Workshop, Neural Networks for Signal Processing VII, NNSP'97* (pp. 406–415). New York: IEEE Press.

Lee, T.-W., Lewicki, M.-S., & Sejnowski, T.-J. (1999). Unsupervised classification with non-Gaussian mixture models using ICA. *Advances in Neural Information Processing Systems*, *11*, 508–514.

Mallat, S. G. (1989). A theory for multiresolution signal decomposition: The wavelet representation. *IEEE Transactions on Pattern Analysis and Machine Intelligence*, *11*, 674–693.

Mika, S., Schölkopf, B., Smola, A., Müller, K.-R., Scholz, M., & Rätsch, G. (1999). Kernel PCA and de-noising in feature spaces. *Advances in Neural Information Processing Systems*, *11*, 536–542.

Müller, K.-R., Mika, S., Rätsch, G., Tsuda, K., & Schölkopf, B. (2001). An introduction to kernel-based learning algorithms. *IEEE Transactions on Neural Networks*, *12*(2), 181–201.

Pajunen, P., Hyvärinen, A., & Karhunen, J. (1996). Nonlinear blind source separation by self-organizing maps. *Progress in Neural Information Processing: Proceedings of ICONIP'96*, Hong-Kong (pp. 1207–1210).

Schölkopf, B., Mika, S., Burges, C. J. C., Knirsch, P., Müller, K.-R., Rätsch, G., & Smola, A. J. (1999). Input space versus feature space in kernel-based methods. *IEEE Transactions on Neural Networks*, *10*, 1000–1017.

Schölkopf, B., Mika, S., Smola, A. J., Rätsch, G., & Müller, K.-G. (1998). Kernel PCA pattern reconstruction via approximate pre-images. In M. Bodn, L. Niklasson, & T. Ziemke (Eds.), *Perspectives in Neural Computing: Proceedings of the 8th International Conference on Artificial Neural Networks* (pp. 147–152). Berlin: Springer.

Schölkopf, B., Smola, A. J., & Müller, K.-R. (1999). Nonlinear component analysis as a kernel eigenvalue problem. *Neural Computation*, *10*, 1299–1319.

Taleb, A., & Jutten, C. (1997). Nonlinear source separation: The post-nonlinear mixtures. *Proceedings of European Symposium on Artificial Neural Networks, ESANN'97*, Bruges, Belgium, April 1997 (pp. 279–284).

Taleb, A., & Jutten, C. (1999). Source separation in postnonlinear mixtures. *IEEE Transactions on Signal Processing*, *47*(10), 2807–2820.

Tan, Y., Wang, J., & Zurada, J. M. (2001). Nonlinear blind source separation using a radial basis function network. *IEEE Transactions on Neural Networks*, *12*(1), 124–134.

Villmann, T., Der, R., Herrmann, M., & Martinetz, T. M. (1997). Topology preservation in self-organizing feature maps: Exact definition and measurement. *IEEE Transactions on Neural Networks*, *8*(2), 256–266.

Weyrich, N., & Warhola, T. (1998). Wavelet shrinkage and generalized cross validation for image denoising. *IEEE Transactions on Image Processing*, *7*(1), 82–90.

Yang, H. H., Amari, S., & Cichocki, A. (1997). Information back-propagation for blind separation of sources in non-linear mixture. *Proceedings of IEEE ICNN'97* (pp. 2141–2146).